Lawrence Berkeley National Laboratory

Title
Influence of wettability and permeability heterogeneity on miscible CO2 flooding efficiency

Permalink
https://escholarship.org/uc/item/4wm7m80t

Authors
Bikkina, Prem
Wan, Jiamin
Kim, Yongman
et al.

Publication Date
2016-02-01

DOI
10.1016/j.fuel.2015.10.090

Peer reviewed

# Influence of wettability and permeability heterogeneity on miscible CO_2 flooding efficiency

Prem Bikkina [1], Jiamin Wan *, Yongman Kim, Timothy J. Kneafsey, Tetsu K. Tokunaga

Earth Sciences Division, Lawrence Berkeley National Laboratory, 1 Cyclotron Road, Berkeley, CA 94720, United States

HIGHLIGHTS

- Significant influence of wettability on CO_2 enhanced oil recovery is revealed.
- High permeability streaks can make CO_2 flooding very inefficient.
- Huff & Puff method may produce significant CO_2 EOR from heterogeneous reservoirs.

GRAPHICAL ABSTRACT
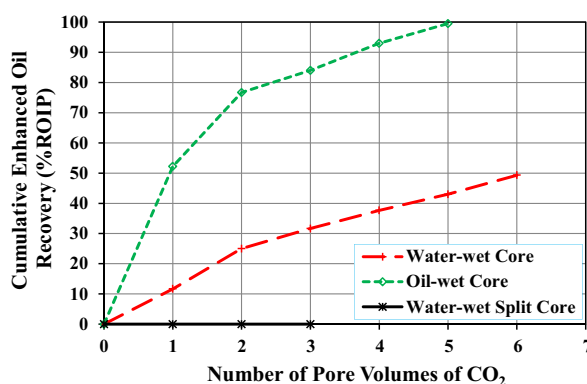
ABSTRACT

CO_2 flooding is a proven enhanced oil recovery (EOR) technique and is also considered as a potential method for CO_2 sequestration. Despite having successful field trials on CO_2 EOR, the effects of reservoir wettability and permeability heterogeneity on the efficiency of miscible CO_2 flooding are not well understood. In this work, laboratory investigations have been carried out to evaluate the influence of these properties on the miscible CO_2 EOR performance. The wettability of hydrophilic Berea core samples was altered to be oil-wet by vacuum saturation of the clean and dry core samples with n-hexadecane. The permeability heterogeneity was obtained by combining two half pieces of axially split water-wet core samples of different permeabilities. Core flooding experiments were conducted for n-hexadecane – synthetic brine – CO_2 systems at 1400 psig backpressure to achieve minimum miscibility pressure (MMP) of CO_2 in n-hexadecane at the test temperature (24 ± 1 °C). It was found that wettability strongly influences CO_2 EOR. For the alternate cases of previously brine flooded (to remaining oil saturation) oil-wet and water-wet core samples, five pore volumes (PVs) of CO_2 recovered 100% and only 43% of remaining oil in place (ROIP) respectively. Three PVs of CO_2 could recover only about 0–5% ROIP from the split core samples. The mechanisms underlying these results are discussed. This study sheds light on the significant influence of reservoir wettability and permeability heterogeneity on the performance of miscible CO_2 EOR.

© 2015 Elsevier Ltd. All rights reserved.

1. Introduction

Wettability is the relative affinity of a fluid to an inert solid substrate in the presence of another immiscible or sparingly soluble fluid [1]. The wettability of petroleum reservoirs may range from

* Corresponding author. Tel.: +1 510 486 6004; fax: +1 510 486 7152.
  E-mail addresses: prem.bikkina@okstate.edu (P. Bikkina), jwan@lbl.gov (J. Wan).
  [1] Present address: School of Chemical Engineering, 224 Cordell North, Oklahoma State University, Stillwater, OK 74078, United States.

strongly water-wet to strongly oil-wet, depending upon the reservoir rock mineralogy, chemistry of the fluids present, and the subsurface pressure and temperature. There are more oil-wet reservoirs in the world compared to water-wet reservoirs [2,3]. Wettability is a major factor that controls multiphase fluid flow, location and distribution of fluids in a reservoir [3]. It has been well recognized that reservoir wettability significantly influences oil production during primary, secondary, and tertiary recovery (enhanced oil recovery) stages [4–6].

The primary recovery stage occurs when the reservoir fluids (mostly oil) are produced using the natural pressure energy available in the reservoir. The secondary recovery stage starts when the pressure in the reservoir declines to such a level that can no longer produce reservoir fluids at the desired rate. Waterflooding is the most widely used secondary recovery method where water or brine is injected into the reservoir through injection wells in order to increase the reservoir pressure so that the reservoir fluids are produced at producing wells. Natural gas re-injection is another secondary recovery method in which the working principle is to increase the reservoir pressure and also to reduce the viscosity of the producing fluid. Gas lift is a commonly used artificial lift method (that may be used with any stage of the oil recovery methods) where the gas is injected into the tubing through tubing-casing annulus to lower the hydrostatic head of the fluids in the tubing so that they could be produced at the desired rate using the available reservoir pressure. Unlike in the gas re-injection method, in gas lift method the gas is not injected into the reservoir and hence the reservoir pressure is not increased.

Typical primary recovery ranges from 5% to 20% of the initial oil in place (IOIP) and secondary recovery adds an additional 10–20% IOIP [7]. Normally, the end point of the secondary recovery would be determined by the economics of the project. About 60–70% of the IOIP is usually left in the reservoir after the secondary recovery. Most of the remaining oil after the secondary recovery is primarily trapped by capillary forces [8]. The capillary forces arise from the fact that oil and water phases present in the reservoir are immiscible and hence an interface forms between the fluid phases. The capillary pressure is controlled by the interfacial tension between the oil and aqueous phases, relative wettability of the reservoir rock to the fluids, and the pore size (distribution) of the rock formation. The effect of capillary forces on oil trapping can be characterized by the Capillary number (N_{Ca}), which is defined as the ratio of viscous to capillary forces [9].

$N_{Ca} = \frac{v\mu}{\sigma cos\theta}$, where, v and μ are the velocity and viscosity of the displacing fluid respectively, σ is the interfacial tension between the oil and water, and θ is the contact angle that quantifies wettability. Significant improvement in oil recovery after the secondary recovery requires the Capillary number to be increased by a factor of 4–6 orders of magnitude [9]. That may be achieved by one or more of the following ways: significantly increasing the velocity and/or viscosity of the displacing fluid; significantly decreasing the oil–water interfacial tension and/or by significantly altering the reservoir wettability. Tertiary recovery methods, for example thermal enhanced oil recovery (TEOR) and chemical enhanced oil recovery (CEOR), target to influence one or more of the above parameters for improved oil recovery. Steam assisted gravity drainage (SAGD) and in-situ combustion are typical TEOR methods and they mainly target to lower the viscosity of the producing oil (displaced fluid) [10,11]. Alkaline–surfactant–polymer (ASP) flooding is a CEOR method that aims to improve the interfacial properties to reduce the capillary barrier and also to increase the viscosity of the displacing fluid for mobility control [12,13].

In the recent decades CO_2 flooding has gained substantial attention as a tertiary recovery method that also simultaneously allows sequestering a portion of the injected CO_2. CO_2 enhanced oil recovery (CO_2 EOR) aims to improve the interfacial properties as well as to reduce the oil viscosity by swelling it. A major disadvantage of CO_2 EOR comes from the very low viscosity of CO_2. The low viscosity promotes viscous fingering and hence very low sweep efficiency. In general, higher sweep efficiencies can be obtained by reducing the mobility ratio (M) which may be defined as,

$$M = \left(\frac{k}{\mu}\right)_{displacing\ phase} \bigg/ \left(\frac{k}{\mu}\right)_{displaced\ phase}$$

where k is the end point relative permeability to the fluid and μ is the fluid viscosity. To avoid viscous fingering and early breakthrough of the displacing fluid, viscosity of the displacing fluid phase should be sufficiently high.

In recent years considerable research efforts have also been devoted to develop CO_2 foams for EOR and hydraulic fracturing applications [14–18]. CO_2 foam flooding has all the advantages of CO_2 flooding and in addition the low viscosity problem is mostly solved as the stable CO_2 foams have few orders of magnitude higher viscosities. Nonetheless, obtaining stable CO_2 foams at reservoir conditions is a real challenge. Therefore, for reasonably homogeneous and low viscosity crude oil reservoirs CO_2 flooding may be a viable option for EOR. Various aspects of CO_2 flooding efficiency have been addressed using laboratory, field scale, and computer simulation studies [18–23].

The flooded CO_2 can be immiscible or miscible with the oil in the reservoir. The CO_2 miscibility with the oil would be primarily determined by the reservoir pressure, temperature, and physico-chemical properties of the oil. The minimum pressure at which CO_2 is miscible in all proportions with the oil at reservoir temperature is referred as the minimum miscibility pressure (MMP). In general, immiscible CO_2 flooding is inefficient in obtaining significant EOR compared to miscible CO_2 flooding [24]. The CO_2 miscibility with oil helps in two primary ways: one, the interface between displacing fluid (CO_2) and displaced fluid (oil) would vanish and hence the corresponding capillary force would become zero; two, due to CO_2 dissolution the oil swells and its viscosity is considerably reduced.

Both the miscible and immiscible CO_2 flooding could be conducted either as a continuous gas injection (CGI) mode or water alternating gas (WAG) injection mode [25]. As the names suggest, in CGI mode CO_2 is continuously injected, whereas in WAG mode water (or brine) and CO_2 are alternately injected. The advantages of WAG injection mode are to reduce the usage of expensive CO_2, and also to limit the viscous fingering of CO_2 through thin high permeability zones ('thief zones') and gravity override issues that are usually encountered in the CGI mode flooding. However, the negative aspect of WAG flooding is that water could make some of the oil unavailable to be contacted by CO_2 (this phenomenon is referred as water blocking) that would reduce the efficiency of the flooding process. Loss of injectivity and corrosion problems are also some other concerns associated with the WAG injection process [26,27].

The wettability of a petroleum reservoir might be anywhere between strongly water-wet to strongly oil-wet, depending upon its mineralogy and physicochemical properties of the fluids. Even an initially strongly water-wet reservoir may become mixed-wet (different wetting preferences at different locations in the reservoir), intermediate-wet (equal preference to oil and water) or oil-wet, during the production period, due to the injected solvents and/or surface active components [4]. The wettability alteration can also result from deposition of natural surface active components such as asphaltenes and resins as a consequence of the reduction in reservoir pressure and/or the decrease in lower

molecular weight hydrocarbons in the reservoir and/or the crude oil interaction with the injected solvents [28].

The effect of wettability on waterflooding is well studied [29]. It is generally recognized that the efficiency of waterflooding in a uniformly water-wet reservoir is higher than that of a uniformly oil-wet reservoir [4,6,29]. However, it was also reported by Rao et al. that the efficiency of waterflooding is highest in mixed-wet reservoirs, followed by intermediate-wet, water-wet and lowest in oil-wet reservoirs [6].

From their ethane miscible flooding experimental results, Rao et al. concluded that the miscible flooding efficiency (% ROIP) is the highest in oil-wet samples, followed by intermediate-wet and mixed-wet and the lowest in water-wet samples [6].

The effect of wettability on miscible CO_2 flooding efficiency has been rarely studied despite its huge technical importance and economic potential in obtaining significant EOR from reservoirs across the world. Hence, this work attempts to fill the gap by conducting systematic miscible CO_2 flooding experiments in CGI mode using water-wet and oil-wet sandstone core samples. All other petrophysical properties of the core samples were similar to one another given the fact that they were twin cores (as explained in the experimental section they were prepared from the same source rock). This study also includes the effect of permeability heterogeneity (introduced in the form of longitudinally split cores) on the miscible CO_2 flooding efficiency.

2. Chemicals and materials

Chemicals and materials used in this study and their purity and sources are given below. CO_2 (99.9%, Praxair), n-Hexadecane (99%, Alfa Aesar), acetone (ACS grade, BDH), KI (99%, Alfa Aesar), NaCl (ACS grade, Sigma–Aldrich), annealed nickel foil (thickness: 0.0125 mm; purity: 99%; Goodfellow Corporation), Teflon film (thickness: 0.0127 mm; ePlastics), Teflon sheet (thickness: 1.016 mm; ePlastics), Berea sandstones (Berea Sandstone Petroleum Cores).

3. Experimental facility

A high pressure, moderate temperature core flooding facility was built for CO_2 and CO_2 foam flooding experiments. The flow diagram of the experimental facility is shown in Fig. 1. The experimental facility constitutes a Hassler type titanium core holder (8000 psi and 200 °C rated) and three Teledyne Isco syringe pumps (models 500D and 500HP of 5000 psi rating; model 65D of 20,000 psi rating) for controlling confining, pore and backpressures during the experiment. Three 316 stainless steel transfer cylinders (two of them were movable piston type) were connected to the pumps for storing and flowing the three test fluids (oil, CO_2, and brine). Two absolute pressure transducers (Omega Engineering, PX309-2KG5V) and a differential pressure transducer (Omega Engineering, PX509HL-050DWB10V-S) were installed for core sample inlet, outlet, and differential pressure measurement. The core holder system contains axial inlet and outlet pore fluid lines with corresponding pressure ports, and two radial ports for confining fluid entry and its pressure measurement. De-ionized water was used as confining fluid and the 65D Teledyne Isco pump was used for the confining pressure. The core holder outlet fluid flow line was connected to a backpressure regulator (BPR) whose pressure was also controlled by the same 65D Teledyne Isco pump. The experiments were conducted at room temperature (24 ± 1 °C). The produced fluids were collected using a fraction collector (Spectrum, Spectra/Chrom CF-1). After aqueous fluid breakthrough during the brine flooding step and also during the early CO_2 flooding, some of the produced fluids were in the form of emulsion and hence a centrifuge (IEC, Centra MP4) was used to separate the oil and aqueous phases.

4. Experimental procedure

A Berea sandstone core sample whose dimensions, porosity, permeability and wettability data are given in Table 1 was wrapped in a layer of nickel foil, two layers of Teflon film, and
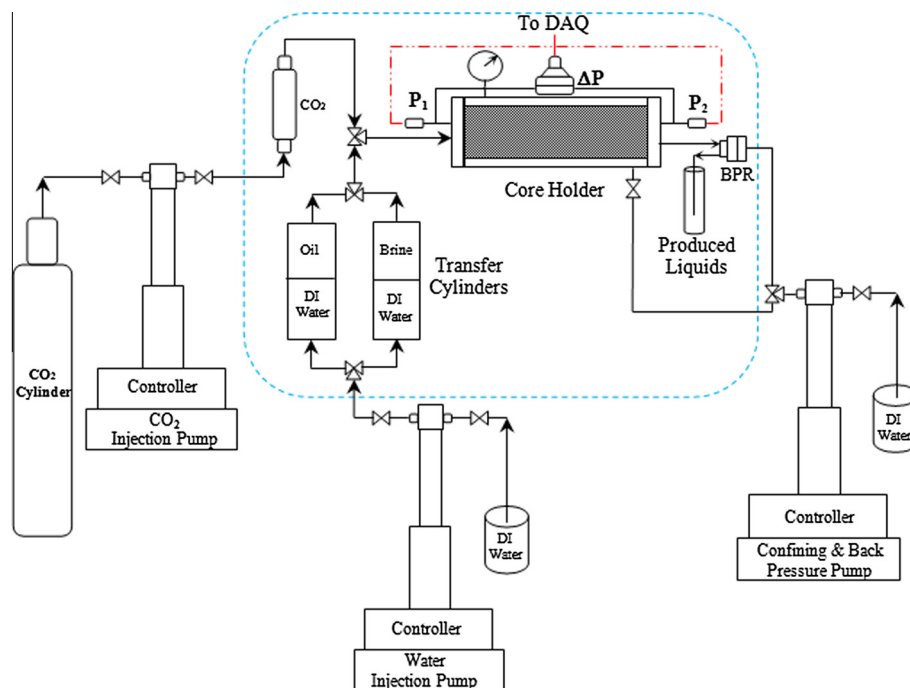

**Fig. 1.** Flow diagram of the coreflooding system.

Table 1
Petrophysical properties of the core samples.

Core	Length (cm)	Diameter (cm)	Porosity (%)	Permeability (mD)
FC#1.1	12.6	3.82	21.6	103.1
FC#1.2	12.4	3.82	21.2	110.0
SC#2.1	13.3	1.92	18.1	28.3
SC#2.2	13.3	1.84	18.1	28.3
SC#2.3	13.3	1.92	18.4	20.5
SC#2.4	13.3	1.82	18.4	20.5
SC#3.1	13.3	1.92	22.2	56.9
SC#3.2	13.3	1.84	22.2	56.9
SC#3.3	13.3	1.93	21.7	51.7
SC#3.4	13.3	1.82	21.7	51.7

placed in a Viton sleeve which was then installed in the core holder. Fig. 2a shows a typical core sample with the nickel and Teflon layers. The multiple layers were required to prevent any CO_2 diffusion through the Viton sleeve. The same procedure was followed for the axially split core (hereafter SC) samples but, a Teflon sheet was placed between the two pieces to prevent any sig-
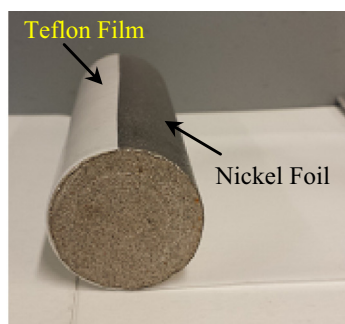
(a)
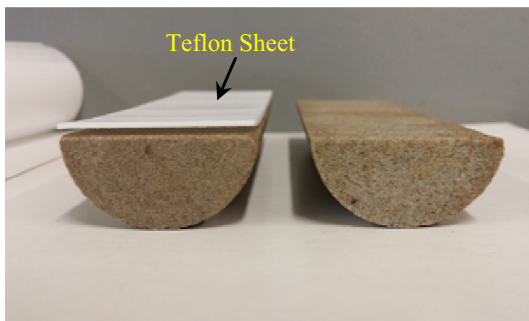
(b)

(c)

Fig. 2. (a) Full core sample wrapped in nickel and Teflon layers, (b) split core sample with the Teflon sheet and (c) split core sample wrapped in nickel and Teflon layers.

nificant by-passing of the cleaning and later the process pore fluids. Photographs of the split core samples are shown in Fig. 2b and c.

Once a core sample was tightly placed between the fixed and movable end pieces of the core holder, a confining pressure of 600 psig was applied in the annular space between the core holder and the sleeve. Then the core sample was flushed with acetone until clear effluent was observed. About 15 pore volumes (PVs) of acetone were used for each core. Then the confining pressure was released and the core was carefully removed from the sleeve, unwrapped from the Teflon and nickel layers and placed in an oven at 110 °C until constant mass was reached.

The cleaned and dried core sample was weighed for its dry mass and then vacuum saturated with an aqueous solution of 0.1 M NaCl (full core samples) or 0.1 M KI (SC samples), until constant mass was reached. In the case of SC samples, each of the two pieces was separately measured for its dry and saturated masses. The PV and porosity of the core sample were measured using the conventional saturation method.

The brine saturated full core (hereafter, FC) sample was prepared and installed in the core holder following the previously mentioned procedure. Then a confining pressure of about 600 psig was applied. Brine flooding was carried out to make sure that the core sample was completely saturated with the brine as well as to measure the absolute permeability of the core. The core was kept in the core holder with the confining pressure for overnight. Then the confining pressure was increased to 1800 psig and the backpressure was set at 1400 psig. The backpressure was chosen so that the CO_2 would be completely miscible with the oil phase (n-hexadecane) at the test temperature (24 ± 1 °C) [30]. Absolute permeability of the core sample at the test, confining and backpressures was measured while flowing few more PVs of the brine. Measured porosities and permeabilities of all the core samples used in this study are reported in Table 1. It should be noted here that the confining pressure increased from 1800 psig to about 1950 psig in response to the pore pressure increase due to the 1400 psig backpressure.

Oil flooding was carried out at the mentioned confining and backpressures and at a flow rate of 0.5 cc/min. The flow rate was chosen to comply with the Rapoport and Leas criteria ($LV\mu \geqslant 1.0$ through 5, where L is the length of the core in cm, V is the displacing fluid velocity in cm/min, and μ is the displacing phase viscosity in cP) for making sure that the displaced fluid recoveries were independent of flow rate [31,32].

Oil flooding was continued until no more brine was displaced from the core sample. The brine saturation at this stage is referred to as the irreducible brine saturation (S_{wir}). The effluent fluids displaced from the core were continuously collected using the fraction collector. From the initial volume of the brine (PV itself) and the brine displaced during the oil flooding, S_{wir} is calculated. The system was kept at the condition for about 18 h and then the flow was switched to brine (0.5 cc/min flow rate) to displace the oil. The brine flooding was continued until no more oil was produced. The oil saturation at that point is referred to as the remaining oil saturation (S_{or}).

Once the remaining oil saturation was reached, the coreflooding system was prepared for CO_2 flooding step. CO_2 was injected at a flow rate of 0.5 cc/min and the volume of oil collected for each PV of CO_2 was recorded. The flooding was continued till 5–6 PVs of CO_2 were injected.

The same procedure was followed for the SC samples except for one critical step mentioned below. After a SC (for example; SC#2.1–2.2) reached remaining oil saturation, the backpressure and confining pressure were slowly reduced to atmospheric pressure. Then the core sample was carefully removed from the core holder and unwrapped. A piece of the SC was then joined with

another similarly prepared SC piece (for example, as shown in Table 1, SC#2.1 was joined with the SC#3.2) with a Teflon sheet between the two pieces. This step was done to prepare a 'Janus core' sample (a SC sample having different permeabilities for each hemicylindrical piece of the core). The Janus core sample was installed in the core holder, and the confining and backpressures were applied. The brine flooding was then continued to increase the pore pressure close to backpressure before starting the CO_2 flooding step.

The FC#1.1 was initially saturated with the oil for about 24 h unlike FC#1.2 and SC samples that were initially saturated with the brine. This was done to make the sample oil-wet. Then the permeability of the core sample was measured by flowing the oil through it. After the permeability measurement step, the core

Spontaneously imbibed water droplets

(a)
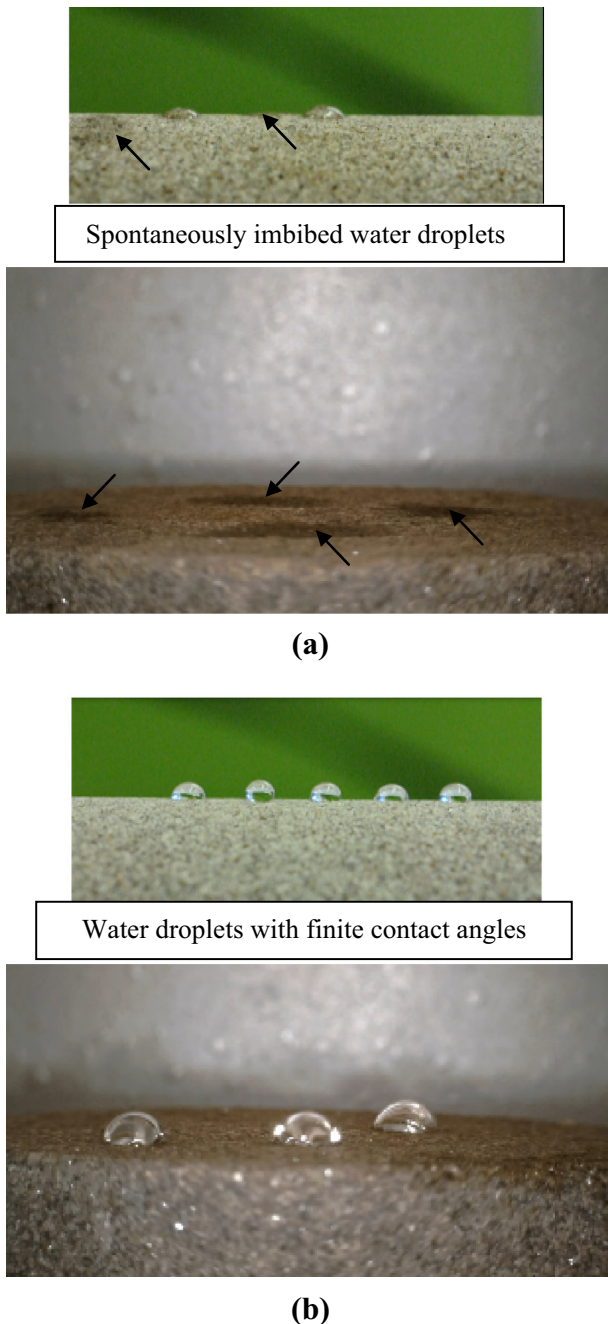
Water droplets with finite contact angles

(b)

Fig. 3. Photographs of water droplets on the radial and axial surfaces of (a) water-wet (FC#1.2) and (b) oil-wet (FC#1.1) core samples.

was brine flooded to remaining oil saturation. The brine flooding was followed by the CO_2 flooding.

The FC#1.1 was used for three experiments and FC#1.2 was used for two experiments. All the SCs were used for one experiment each.

5. Experimental results and discussion

5.1. Effect of wettability

After the first set of coreflood experiments using FC#1.1 (initially wetted by oil) and FC#1.2 (initially wetted by brine), the cores were flushed using about 15 PVs of acetone and dried in the oven at 110 °C. Then, 5 μl DI water droplets were placed on axial and radial surfaces of the samples. As shown in Fig. 3a and b, most of the droplets placed on the FC#1.2 were spontaneously imbibed into the core and all the droplets placed on the FC#1.1 were beaded up and did not imbibe into the core within the 5 min test duration. This indicates direct contact of the initially cleaned core sample with oil altered the wettability of the originally water-wet rock sample toward oil-wetting nature. The altered wettability could not be restored to the original strongly water-wet state even by flushing the core sample using copious amount of acetone, possibly because of the strongly adsorbed oil layer on the rock surface. The water film on the FC#1.2 apparently prevented the adsorption of the oil on the rock surface.

Fig. 4 shows an example of pressure drop across the length of a sample core vs. time trends measured using the two absolute pressure transducers and the differential pressure transducer, at different flow rates. The close match between the two pressure drop profiles attests to the efficacy of the transducers used. Temporal evolution of the pressure drop during the brine flooding, and CO_2 flooding stages of the FC#1.1 are reported in Fig. 5a and b. Fig. 5a shows the pressure drop data during the brine flooding of the three separate experiments conducted using the core sample and Fig. 5b shows the corresponding pressure drop data for the CO_2 flooding. As can be seen in the Figures, pressure drop data agree well among the three experiments. In the 2nd experiment of the FC#1.1, a small leak was observed during the 2nd PV of the CO_2 flooding. Therefore, only the data collected during the 1st PV is used for data analysis. During the 3rd experiment on the core, Joule–Thompson cooling was observed on the BPR leading to a slight malfunctioning of the BPR from freezing and some oscillations in the outlet and inlet pressures.

Fig. 6a–c shows the temporal evolution of the pressure drop data during the oil flooding, brine flooding, and CO_2 flooding of the FC#1.2, respectively. As can be seen in the figures, the pressure
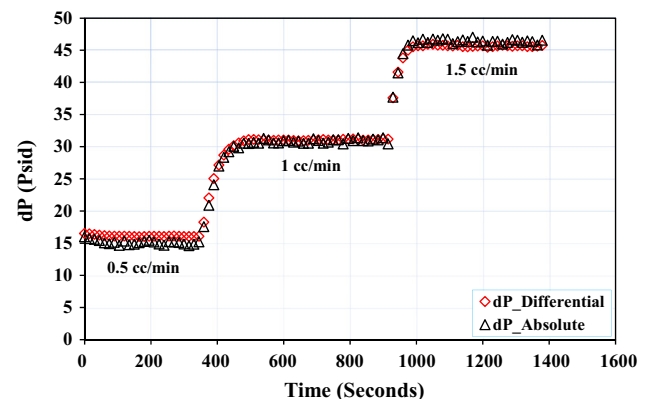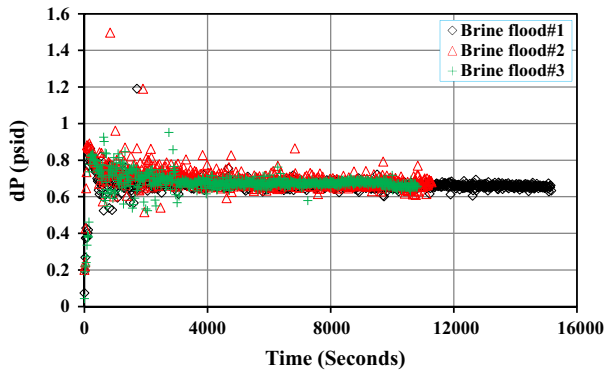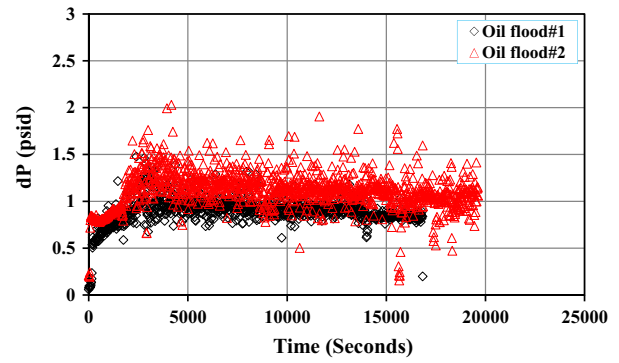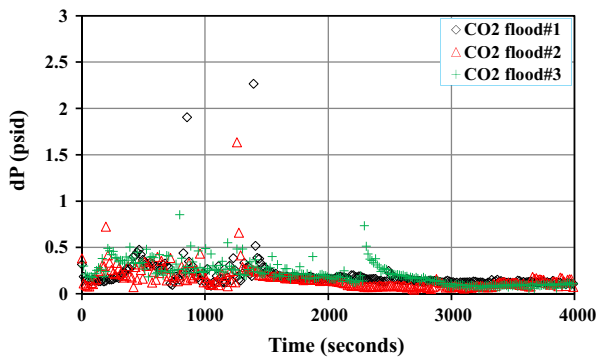

Fig. 4. Pressure drop profiles along the length of a sample core measured using absolute and differential pressure transducers.
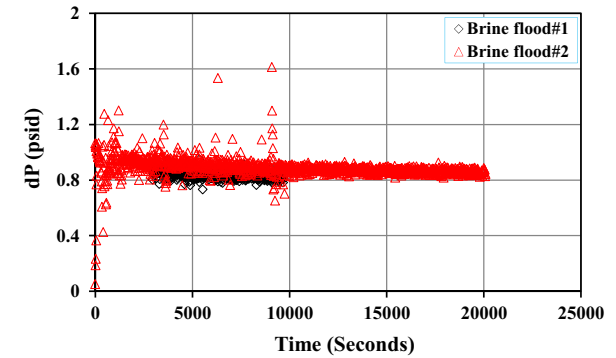
Fig. 5. Pressure drop vs. time profiles of FC#1.1 (oil-wet core) during (a) brine flooding and (b) CO_2 flooding experiments 1–3.

drops are slightly higher in the case of 2nd experiment. The increase in the pressure drops may be attributed to the change in the wettability in some portions of the sample, possibly due to adsorption of oil at those locations during the previous (1st) experiment. This is consistent with the observation that after the first experiment with the core (FC#1.2), water droplets at few locations on the core took time to imbibe. That means at those locations the core became relatively hydrophobic.

The measured irreducible brine and remaining oil saturation data of FC#1.1 and FC#1.2 are given in Tables 2, 3a and 3b. From Table 2, it can be observed that the irreducible brine saturation of FC#1.2 decreased by about 2.4% IOIP from experiments 1 to 2. The decreased irreducible brine saturation also suggests that the wettability of the core might have been slightly altered toward oil-wet before the experiment 2. The increase in the remaining oil saturation (Table 3b) by about 5.9% IOIP from the experiments 1 to 2 also strengthens the above inference.

As reported in Table 3a, average remaining oil saturation of the oil-wet core (FC#1.1) is 92.2% IOIP with a standard deviation of 2.6%. The remaining oil saturation of the oil-wet core (FC#1.1) is about 40% IOIP higher than that of the water-wet core (FC#1.2, Table 3b). This result is consistent with the current understanding of waterflooding efficiency trends of water-wet and oil-wet reservoirs. These controlled experiments revealed the huge influence of wettability on the oil recovery during brine flooding. Thus, the actual oil left for CO_2 EOR is much higher in the case of FC#1.1 (oil-wet core) compared to the FC#1.2 (water-wet core). Above 50% of the ROIP of the FC#1.1 that could not be recovered during the brine flooding was recovered by the 1st PV of CO_2 flooding which can be observed in Fig. 7. In the case of the oil-wet core, 5 PVs of CO_2 recovered nearly 100% ROIP (about 92% IOIP), whereas
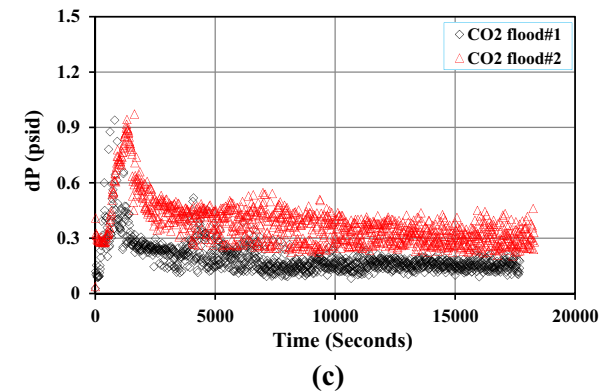
Fig. 6. Pressure drop vs. time trends in FC#1.2 (water-wet core) during (a) oil flooding, (b) brine flooding and (c) CO_2 flooding experiments 1 and 2.

in the case of water-wet core, the same 5 PVs of CO_2 recovered only 43% of ROIP that corresponds to about 33% IOIP.

The very significant difference between the miscible CO_2 flooding efficiencies in the lab scale water-wet and oil-wet core samples reflects several processes. Most probably the remaining oil available in the water-wet core after the brine flooding step could be in the form of discontinuous ganglia at the pore scale and/or

Table 2
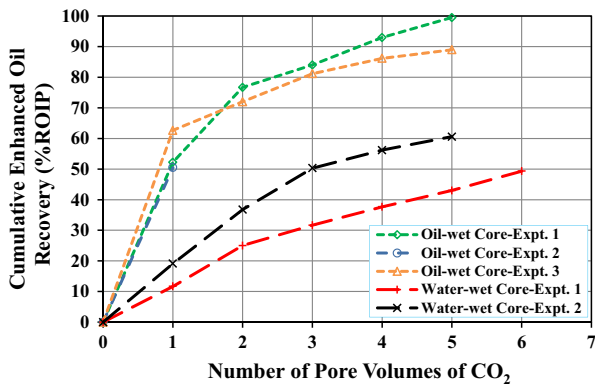Oil flooding data of FC#1.2 (water-wet core).

Oil flooding – FC#1.2	Experiment#1	Experiment#2
Brine collected (cc)	24	25
Dead volume (cc)	4.32	4.32
Brine displaced from the core (cc)	19.68	20.68
Irreducible brine saturation (% IOIP)	34.36	31.95
Initial oil in place, IOIP (cc)	19.68	20.68

Table 3a
Brine flooding data of FC#1.1 (oil-wet core).

Brine flooding – FC#1.1	Experiment#1	Experiment#2	Experiment#3
Oil collected (cc)	7	6	7.75
Dead volume (cc)	4.32	4.32	4.32
Oil displaced from the core (cc)	2.68	1.68	3.43
Remaining oil saturation (% IOIP)	91.96	94.96	89.71
Remaining oil in place (cc)	30.64	31.64	29.89
Brine in the core (% PV)	8.04	5.04	10.29
Oil recovered (% IOIP)	8.04	5.04	10.29

Table 3b
Brine flooding data of FC#1.2 (water-wet core).

Brine flooding – FC#1.2	Experiment#1	Experiment#2
Oil collected (cc)	9	8
Dead volume (cc)	4.32	4.32
Oil displaced from the core (cc)	4.68	3.68
Remaining oil saturation (% IOIP)	50.03	55.94
Remaining oil in place (cc)	15.00	17.00
Brine in the core (% PV)	49.97	44.06
Oil recovered (% IOIP)	23.78	17.79

Table 4
CO_2 EOR from the split core samples.

Janus core	Remaining oil after brine flooding (% IOIP)	EOR from 3 PVs of CO_2 (% ROIP)
SC#2.1–3.2	61.6	0
SC#2.2–3.1	60.9	0
SC#2.3–3.4	70.3	5.05
SC#2.4–3.3	69.7	0

Fig. 7. Enhanced oil recovery during CO_2 flooding in oil-wet (FC#1.1) and water-wet (FC#1.2) Cores.
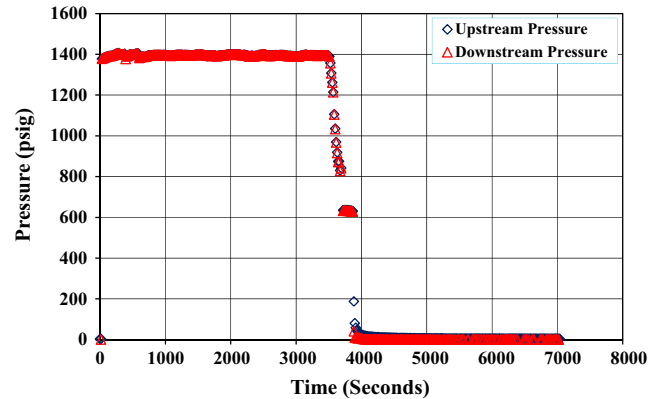
Fig. 8. (a) Absolute pressure and (b) differential pressure responses during the backpressure reduction to atmospheric pressure.
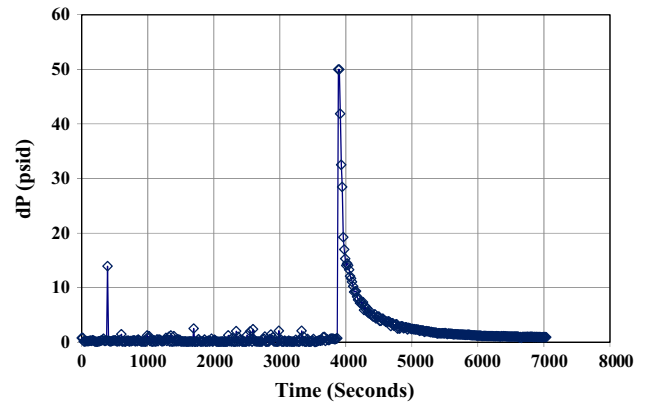
blocked by the flooded brine at the core scale (typical water blocking phenomena). In either of the cases, the injected CO_2 for tertiary recovery would have to first dissolve in the continuous brine phase in order to reach and dissolve in the discontinuous oil blobs. This process would be limited by the interphase mass transfer of CO_2 through the water–oil interface. Even if CO_2 is able to dissolve in some or all of the oil blobs, the corresponding swelling of the oil ganglia may not be sufficient to make the remaining oil a continuous phase to be produced. However, if sufficient amount of CO_2 is flooded for sufficiently longer period all of the trapped oil will be produced, but, the process may not be economically feasible. The above reasoning is also strengthened by the significantly higher secondary recovery (about 50% of the IOIP) in the water-wet core compared to the oil-wet core (less than 10% of the IOIP). Higher brine saturation of the core increases the probability for the oil to become a discontinuous phase and/or blocked by the brine. With the same reasoning, one can speculate that the oil is still a continuous phase after the secondary recovery in the oil-wet core. So, CO_2 can directly dissolve in the continuous oil phase and produce it. We are currently in the process of testing this hypothesis by conducting similar coreflooding experiments in a microCT scanner.

5.2. Effect of permeability heterogeneity

As explained in the experimental section, split core pieces of the same core were first vacuum saturated with brine, flooded with oil to S_{wir}, and then flooded with brine to S_{or}. Then a piece of the split core was joined with a piece of another similarly prepared split core to prepare a Janus core sample, which was at the remaining oil saturation, for CO_2 flooding. Four Janus split cores were prepared and used for CO_2 flooding. The S_{or} data of the Janus split cores are given in Table 4.

As shown in the Table 4, no oil was recovered during the 3 PVs of CO_2 flooded through three of the four Janus split core samples and for the fourth core sample, only about 5% of the ROIP after the brine flooding was recovered. That implies CO_2 preferentially flowed through the purposely created high permeability longitudinal split. However, when the backpressure was slowly reduced to atmospheric pressure, while the CO_2 injection had been stopped, about 44% and 25% of ROIP was produced from the Janus cores SC#2.2–3.1 and SC#2.4–3.3, respectively. The above process is

analogous to the well-known Huff & Puff CO_2 EOR method. This result indicates that enough CO_2 entered into the rock matrix and dissolved in the ROIP, even though the CO_2 was not able to bring oil out of the matrix during the continuous CO_2 flooding. However, when the backpressure was slowly reduced to atmospheric pressure, the dissolved CO_2 evolved out of the oil and forced the oil to produce from the matrix. The absolute and differential pressure responses in the SC#2.2–3.1 during the backpressure reduction can be observed in the Fig. 8a and b respectively. In fact, the 3rd PV of CO_2 injection was carried out after an overnight soaking period. As mentioned in the Table 4, even after the soaking period, the 3rd PV of CO_2 did not recover any oil from the split core. When the backpressure was slowly reduced to atmospheric pressure, while the CO_2 injection was stopped after the 3rd PV, the absolute pressures also slowly reduced to atmospheric pressure as shown in the Fig. 8a. However, the reduction in the backpressure resulted a sudden rise in the pressure drop to about 50 psid that can be observed in the Fig. 8b. The huge pressure drop might be a consequence of the dissolved gas liberation from the oil. The evolved gas might have applied sufficient pressure on the previously immobile oil to produce. The pressure drop declined to negligible levels in about an hour.

6. Conclusions

Controlled coreflood experiments using twin-sandstone core samples revealed the strong effect of wettability on the efficiency of miscible CO_2 EOR process. Miscible CO_2 flooding performed significantly better in the oil-wet cores compared to the water-wet cores. While the miscible CO_2 flooding could perform reasonably well in the case of homogeneous water-wet core and perform excellently in the case of homogeneous oil-wet core, the EOR technique could not achieve any significant improved oil recovery in the case of heterogeneous water-wet core with a fracture (thief zone). In the case of heterogeneous reservoirs, the low viscosity of the CO_2 would divert the fluid through high permeability thief zones and hence results in none to very low flooding efficiencies. Appropriate sweep efficiency improvement methods may be necessary for enhancing oil recovery in heterogeneous water-wet reservoirs.

References

[1] Zinszner B, Pellerin FM. A geoscientist's guide to petrophysics. Editions Ophrys; 2007.
[2] Rao DN, Ayirala SC, Abe AA, Xu W. Impact of low-cost dilute surfactants on wettability and relative permeability. SPE/DOE Symp Improv Oil Recov 2006.
[3] Anderson WG. Wettability literature survey – Part 1: rock/oil/brine interactions and the effects of core handling on wettability. J Petrol Technol 1986;38(11):1125–44.
[4] Nr M. Effect of wettability on waterflood recovery for crude-oil brine rock systems. SPE Reserv Eng 1995;10(1):40–6.
[5] Zhou X, Morrow N, Ma S. Interrelationship of wettability initial water saturation aging time and oil recovery by spontaneous imbibition and waterflooding. SPE J 2000;5(02):199–207.
[6] Rao D, Girard M, Sayegh S. The influence of reservoir wettability on waterflood and miscible flood performance. J Can Pet Technol 1992;31(06):47–55.
[7] Van't Veld K, Phillips OR. The economics of enhanced oil recovery: estimating incremental oil supply and CO_2 demand in the powder river basin. Energy J 2010;31(4):31–56.
[8] Bondor P. Applications of carbon dioxide in enhanced oil recovery. Energy Convers Manage 1992;33(5):579–86.
[9] Ayirala SC, Rao DN. Multiphase flow and wettability effects of surfactants in porous media. Colloids Surf, A 2004;241(1):313–22.
[10] Al Bahlani AMM, Babadagli T. A critical review of the status of SAGD: where are we and what is next? SPE western regional and Pacific section AAPG joint meeting; 2008.
[11] Kovscek A, Castanier LM, Gerritsen M. Improved predictability of in-situ combustion enhanced oil recovery. SPE Reservoir Eval Eng 2013;16 (02):172–82.
[12] Deng S, Bai R, Chen JP, Yu G, Jiang Z, Zhou F. Effects of alkaline/surfactant/polymer on stability of oil droplets in produced water from ASP flooding. Colloids Surf, A 2002;211(2):275–84.
[13] Bikkina P, Uppaluri R, Purkait M. Evaluation of surfactants for the cost effective enhanced oil recovery of Assam crude oil fields. Pet Sci Technol 2013;31 (7):755–62.
[14] Kim J, Dong Y, Rossen WR. Steady-state flow behavior of CO_2 foam. SPE J 2005;10(04):405–15.
[15] Heller JP. CO_2 foams in enhanced oil recovery. Adv Chem Ser 1994;242. pp. 201–201.
[16] Mohd T, Muhayyidin A, Ghazali N, Shahruddin M, Alias N, Arina S, et al. Carbon dioxide (CO_2) foam stability dependence on nanoparticle concentration for enhanced oil recovery (EOR). Appl Mech Mater 2014;548:1876–80.
[17] Enick RM, Olsen DK, Ammer JR, Schuller W. Mobility and conformance control for CO_2 EOR via thickeners foams and gels – a literature review of 40 years of research and pilot tests. SPE Improv Oil Recov Symp 2012.
[18] Tao HS, Sun X. Experimental study on CO_2 foam flooding characteristics. Adv Mater Res 2014;953:1189–95.
[19] Zhao Y, Song Y, Liu Y, Liang H, Dou B. Visualization and measurement of CO_2 flooding in porous media using MRI. Ind Eng Chem Res 2011;50(8):4707–15.
[20] Grigg RB, Schechter DS. Improved efficiency of miscible CO_2 floods and enhanced prospects for CO_2 flooding heterogeneous reservoirs. US Department of Energy, National Petroleum Technology Office, National Energy Technology Laboratory; 2001.
[21] Cao M, Gu Y. Physicochemical characterization of produced oils and gases in immiscible and miscible CO_2 flooding processes. Energy Fuels 2012;27 (1):440–53.
[22] Moreno R, Santos RG, Okabe C, Schiozer DJ, Trevisan OV, Bonet EJ, et al. Comparison of residual oil saturation for water and supercritical CO_2 flooding in a long core, with live oil at reservoir conditions. J Porous Media 2011;14 (8):699–709.
[23] Gao P, Towler B. Integrated investigation of enhanced oil recovery in south Slattery Minnelusa reservoir, Part 2: CO_2 miscible injection. Pet Sci Technol 2012;30(24):2543–51.
[24] Shokir EM, Al-Quraishi AR, Elhomadhi ES. Immiscible and miscible gas–oil displacement in porous media. ARP-25-45, final report, King Saud University; 2008.
[25] Kulkarni MM. Immiscible and miscible gas–oil displacements in porous media. MS Thesis. Lousian State University; 2003.
[26] Sohrabi M, Jamiolahmady M. Mechanism of injectivity loss during water-alternating-gas (WAG) injection. Gas (C1+ nC10) 5(7):0–0209.
[27] Stone P, Steinberg B, Goodson J. Completion design for waterfloods and CO_2 floods. SPE Prod Eng 1989;4(04):365–70.
[28] Kokal S. Crude oil emulsions: a state-of-the-art review. Old Prod Facil 2005;20 (1):5–13.
[29] Anderson WG. Wettability literature survey – Part 6: the effects of wettability on waterflooding. J Petrol Technol 1987;39(12). 1,605–601, 622.
[30] Zolghadr A, Escrochi M, Ayatollahi S. Temperature and composition effect on CO_2 miscibility by interfacial tension measurement. J Chem Eng Data 2013;58 (5):1168–75.
[31] Haugen J. Scaling criterion for relative permeability experiments on samples with intermediate wettability. London, UK: Society of Core Analysts Symposium; 1990.
[32] Rapoport L, Leas W. Properties of linear waterfloods. Trans AIME 1953;198:139–48.